doi:10.1093/brain/awv320 BRAIN 2016: 139; 73–85 | 73

BRAIN
A JOURNAL OF NEUROLOGY

ALS5/SPG11/*KIAA1840* mutations cause autosomal recessive axonal Charcot–Marie–Tooth disease

Celeste Montecchiani,[1] Lucia Pedace,[1] Temistocle Lo Giudice,[1,2] Antonella Casella,[1] Marzia Mearini,[1] Fabrizio Gaudiello,[1] José L. Pedroso,[3] Chiara Terracciano,[2] Carlo Caltagirone,[2,4] Roberto Massa,[2] Peter H. St George-Hyslop,[5,6,7] Orlando G. P. Barsottini,[3] Toshitaka Kawarai[8] and Antonio Orlacchio[1,2]

Charcot–Marie–Tooth disease is a group of hereditary peripheral neuropathies that share clinical characteristics of progressive distal muscle weakness and atrophy, foot deformities, distal sensory loss, as well as diminished tendon reflexes. Hundreds of causative DNA changes have been found, but much of the genetic basis of the disease is still unexplained. Mutations in the ALS5/SPG11/*KIAA1840* gene are a frequent cause of autosomal recessive hereditary spastic paraplegia with thin corpus callosum and peripheral axonal neuropathy, and account for ~40% of autosomal recessive juvenile amyotrophic lateral sclerosis. The overlap of axonal Charcot–Marie–Tooth disease with both diseases, as well as the common autosomal recessive inheritance pattern of thin corpus callosum and axonal Charcot–Marie–Tooth disease in three related patients, prompted us to analyse the ALS5/SPG11/*KIAA1840* gene in affected individuals with autosomal recessive axonal Charcot–Marie–Tooth disease. We investigated 28 unrelated families with autosomal recessive axonal Charcot–Marie–Tooth disease defined by clinical, electrophysiological, as well as pathological evaluation. Besides, we screened for all the known genes related to axonal autosomal recessive Charcot–Marie-Tooth disease (CMT2A2/HMSN2A2/*MFN2*, CMT2B1/*LMNA*, CMT2B2/*MED25*, CMT2B5/*NEFL*, ARCMT2F/dHMN2B/*HSPB1*, CMT2K/*GDAP1*, CMT2P/*LRSAM1*, CMT2R/*TRIM2*, CMT2S/*IGHMBP2*, CMT2T/*HSJ1*, CMTRID/*COX6A1*, ARAN-NM/*HINT* and GAN/*GAN*), for the genes related to autosomal recessive hereditary spastic paraplegia with thin corpus callosum and axonal peripheral neuropathy (SPG7/*PGN*, SPG15/*ZFYVE26*, SPG21/*ACP33*, SPG35/*FA2H*, SPG46/*GBA2*, SPG55/*C12orf65* and SPG56/*CYP2U1*), as well as for the causative gene of peripheral neuropathy with or without agenesis of the corpus callosum (*SLC12A6*). Mitochondrial disorders related to Charcot–Marie–Tooth disease type 2 were also excluded by sequencing *POLG* and *TYMP* genes. An additional locus for autosomal recessive Charcot–Marie–Tooth disease type 2H on chromosome 8q13-21.1 was excluded by linkage analysis. Pedigrees originated in Italy, Brazil, Canada, England, Iran, and Japan. Interestingly, we identified 15 ALS5/SPG11/*KIAA1840* mutations in 12 families (two sequence variants were never reported before, p.Gln198* and p.Pro2212fs*5). No large deletions/duplications were detected in these patients. The novel mutations seemed to be pathogenic since they co-segregated with the disease in all pedigrees and were absent in 300 unrelated controls. Furthermore, *in silico* analysis predicted their pathogenic effect. Our results indicate that ALS5/SPG11/*KIAA1840* is the causative gene of a wide spectrum of clinical features, including autosomal recessive axonal Charcot–Marie–Tooth disease.

1 Laboratorio di Neurogenetica, CERC - IRCCS Santa Lucia, Rome, Italy
2 Dipartimento di Medicina dei Sistemi, Università di Roma "Tor Vergata", Rome, Italy
3 Department of Neurology, Universidade Federal de São Paulo, Brazil
4 Laboratorio di Neurologia Clinica e Comportamentale, IRCCS Santa Lucia, Rome, Italy
5 Centre for Research in Neurodegenerative Diseases, University of Toronto, Toronto, Ontario, Canada
6 Department of Medicine, University of Toronto, Toronto, Ontario, Canada
7 Department of Clinical Neurosciences, University of Cambridge, Cambridge, UK
8 Department of Clinical Neuroscience, Institute of Biomedical Sciences, Tokushima University Graduate School, Tokushima, Japan

Received July 13, 2015. Revised September 3, 2015. Accepted September 21, 2015. Advance Access publication November 10, 2015

Correspondence to: Prof. Antonio Orlacchio,
Laboratorio di Neurogenetica,
Centro Europeo di Ricerca sul Cervello (CERC) -
Istituto di Ricovero e Cura a Carattere Scientifico (IRCCS) Santa Lucia,
64 Via del Fosso di Fiorano,
Rome 00143,
Italy
E-mail: a.orlacchio@hsantalucia.it

Keywords: ALS5/SPG11/*KIAA1840* mutations; axonal degeneration; Charcot–Marie–Tooth disease; spatacsin

Abbreviations: ARCMT2 = autosomal recessive Charcot–Marie–Tooth disease type 2; ARHSP = autosomal recessive hereditary spastic paraplegia; CMT = Charcot–Marie–Tooth

Introduction

Mutations in the ALS5/SPG11/*KIAA1840* gene, located on chromosome 15q21.1, cause autosomal recessive hereditary spastic paraplegia (ARHSP; OMIM #604360), frequently associated with thin corpus callosum and axonal peripheral neuropathy (Stevanin *et al.*, 2007*a*, *b*; Lo Giudice *et al.*, 2014), as well as autosomal recessive juvenile amyotrophic lateral sclerosis (ARJALS; OMIM %602099), characterized by slowly progressive spasticity of limb and facial muscles with distal amyotrophy of hands and feet (Orlacchio *et al.*, 2010). Charcot–Marie–Tooth (CMT) disease is a hereditary peripheral neuropathy characterized by slowly progressive distal muscle weakness, atrophy, and mild sensory loss, primarily in lower limbs. It is the most common degenerative disorder of the peripheral nervous system, with a global prevalence of 1 in 2500 (Tazir *et al.*, 2013). Phenotypes are grouped within the hereditary motor and sensory neuropathies (HMSNs; Dyck and Thomas, 2005) and can be divided into demyelinating (CMT1), axonal (CMT2), and intermediate forms, on the basis of electrophysiological criteria as well as pathological features (Dyck *et al.*, 1968). In CMT2, peripheral nerves are neither enlarged nor hypertrophic, with normal or near-normal conduction velocities; the disease course is highly variable, ranging from mild to severe forms (Feely *et al.*, 2011; Tazir *et al.*, 2014). The subtypes belonging to ARCMT2 share common and distinctive clinical features, e.g. CMT2B2 is characterized by sensory deficits, whereas CMT2K is characterized by hoarse voice and vocal cord paresis (Claramunt *et al.*, 2005; Leal *et al.*, 2009). To date, ARCMT2 has been associated with mutations in only a few genes, and many forms are still unrecognized (Bird, 1993-2015). Recent advances in the molecular genetics of Charcot–Marie–Tooth disease have contributed to the classification and diagnosis of this heterogeneous disease (Jerath and Shy, 2015).

The overlap between CMT2 and hereditary spastic paraplegia (Timmerman *et al.*, 2013; Fridman and Murphy, 2014), as well as the fact that the ALS5/SPG11/*KIAA1840* gene product (spatacsin) is implicated in axonal maintenance and cargo trafficking (Pérez-Brangulí *et al.*, 2014), and the common autosomal recessive inherited findings of thin corpus callosum and CMT2 in three related patients, motivated us to investigate the ALS5/SPG11/*KIAA1840* gene in families with ARCMT2 with no causative gene identified.

Materials and methods

Patients

This study was performed according to a protocol reviewed and approved by the Ethics Committee of the *Istituto di Ricovero e Cura a Carattere Scientifico Santa Lucia*, Rome, Italy. After obtaining informed consent, patients were recruited by a network of neurologists in Italy, Brazil, Canada, England, and Japan, with a significant background in peripheral neuropathy.

The study focused on 28 unrelated pedigrees with ARCMT2 and without genetic assessment. The diagnosis of ARCMT2 was based on neurological findings, familial history, along with neurophysiological characteristics (Bird, 1993-2015). Flexor and extensor muscle strength was assessed manually using the standard Medical Research Council Scale (Medical Research Council, 1981). The Functional Disability Scale and the Charcot–Marie–Tooth Neuropathy Score assessed the staging of the disease (Birouk *et al.*, 1997; Murphy *et al.*, 2011).

All affected subjects under the age of 18 were investigated for IQ through the Wechsler Intelligence Scales for Children IV, including the Wechsler Memory Scale (http://alpha.fdu.edu/psychology/WISCIV_Index.htm). According to the criteria of the Diagnostic and Statistical Manual of Mental Disorders, Fifth Edition (American Psychiatric Association, 2013), mental retardation was considered when the IQ was $\leqslant 70$ before the age of 18. Adults were evaluated by Mental Deterioration Battery (Carlesimo *et al.*, 1996) to assess cognitive impairment. Brain MRI was obtained in all affected individuals, with the exception of eight subjects. Haematological and biochemical profiles, as well as lysosomal enzyme assay of β-hexosaminidase A and B in peripheral blood leucocytes, were performed in at least one patient within each family. CSF analysis was available in 21 patients. Vitamins B_1, B_2, B_6, B_9, B_{12}, and E were measured in all patients.

Nerve conduction study was carried out with a surface skin temperature between 32°C and 34°C. Nerves were analysed

bilaterally in upper and lower limbs using percutaneous stimulation and surface recording electrodes. Concentric needle EMG was performed in muscles of upper and lower limbs: spontaneous activity, duration, and amplitude of motor unit action potentials, as well as motor unit action potentials, interference pattern during maximal voluntary contraction, were recorded.

Sural nerve biopsy was available in 25 patients. Light microscopy preparations, and the electron microscopic analysis in one patient, were performed according to standard methods (Palumbo *et al.*, 2002).

Genetic analyses

Genomic DNA was extracted from peripheral blood using the Promega Wizard® Genomic DNA isolation kit. Linkage study of the 28 families with ARCMT2 was performed using microsatellite markers flanking the ALS5/SPG11 locus, as previously described (Orlacchio *et al.*, 2010). In the probands, all the coding exons of ALS5/SPG11/*KIAA1840* and at least 50 bp of flanking intronic sequence were PCR-amplified by primer pairs, as previously described (Stevanin *et al.*, 2007*a*), and by Roche FastStart™ PCR Master Mix polymerase. All the PCR-amplified products were purified using a Qiagen PCR purification kit. Purified products were sequenced with respective forward and reverse primers by an Applied Biosystems 3130 Genetic Analyzer. Sequence analysis was performed using SeqScape software (v2.6; Applied Biosystems). Large genomic rearrangements of ALS5/SPG11/*KIAA1840* gene were investigated by multiplex ligation-dependent probe amplification method with the P306-B1 SPG11 probe mix, containing probes for each of the 40 *KIAA1840* exons. Data were collected and analysed with GeneScan software (v.3.1.2; Applied Biosystems). For each sample, peak areas were calculated and compared with three wild-type controls, using Coffalyser software (v.7.0; MRC Holland).

The segregation analysis within the family and the surveillance of mutations in the control population were performed using a PCR-restriction fragment length polymorphism method. Three hundred control chromosomes were obtained from healthy volunteers of mixed ethnic origins, including Caucasian, Brazilian and Japanese.

An *in silico* pathogenicity prediction tool (Mutation Taster, http:www.mutationtaster.org) was used to predict the effect of the novel mutations identified, as previously described (Carosi *et al.*, 2015).

In all probands, we performed direct sequencing of all exons and flanking introns of CMT2A2/HMSN2A2/*MFN2* (OMIM: #609260; Nicholson *et al.*, 2008), CMT2B1/*LMNA* (OMIM: #605588; De Sandre-Giovannoli *et al.*, 2002), CMT2B2/*MED25* (OMIM: #605589; Leal *et al.*, 2009), CMT2B5/*NEFL* (OMIM: #607734; Yum *et al.*, 2009), ARCMT2F/dHMN2B/*HSPB1* (OMIM: #608634; Houlden *et al.*, 2008), CMT2K/*GDAP1* (OMIM: #607831; Claramunt *et al.*, 2005), CMT2P/*LRSAM1* (OMIM: #614436; Guernsey *et al.*, 2010), CMT2R/*TRIM2* (OMIM: #615490; Pehlivan *et al.*, 2015), CMT2S/*IGHMBP2* (OMIM: #616155; Cottenie *et al.*, 2014), CMT2T/*HSJ1* (OMIM: #616233; Gess *et al.*, 2014), CMTRID/*COX6A1* (OMIM: #616039; Tamiya *et al.*, 2014), ARAN-NM/*HINT* (OMIM: #137200; Zimoń *et al.*, 2012), GAN/*GAN* (OMIM: #256850; Bomont *et al.*, 2000), SPG7/*PGN* (OMIM: #607259; Casari *et al.*, 1998), SPG15/*ZFYVE26* (OMIM: #270700; Hanein *et al.*, 2008), SPG21/*ACP33* (OMIM: #248900; Simpson *et al.*, 2003), SPG35/*FA2H* (OMIM: #612319; Pierson *et al.*, 2012), SPG46/*GBA2* (OMIM: #614409; Hammer *et al.*, 2013; Martin *et al.*, 2013), SPG55/*C12orf65* (OMIM: #615035; Spiegel *et al.*, 2014), SPG56/*CYP2U1* (OMIM: #610670; Tesson *et al.*, 2012), and *SLC12A6* (OMIM: #604878; Howard *et al.*, 2002). Direct sequencing of *POLG* (OMIM: #174763; Van Goethem *et al.*, 2001) and *TYMP* (OMIM: #131222; Nishino *et al.*, 2000) genes was also carried out to exclude mitochondrial disorders related to CMT2 (Cassereau *et al.*, 2014). Furthermore, linkage to chromosome 8q13-21.1 was performed to investigate autosomal recessive CMT2H, as previously reported (Barhoumi *et al.*, 2001).

Results

Genetic findings

Linkage analysis in 28 unrelated pedigrees with ARCMT2 highlighted homozygous haplotypes with positive logarithm of odds score in all affected subjects from consanguineous parents of nine families (Families RM-501, RM-588, RM-603, RM-626, SP-012, SP-026, TOR-018, TOR-029 and TK-031), showing a cumulative two-point logarithm of odds score of 11.76 at the recombination fraction $\theta = 0.0$ for marker D15S537 (Fig. 1). The other ARCMT2 families showed heterozygous haplotypes and three of these kindred (Families RM-801, RM-888, and CAM-006) had positive logarithm of odds score in all affected individuals, showing a cumulative two-point logarithm of odds score of 6.29 at the recombination fraction $\theta = 0.0$ for marker D15S537 (Fig. 1). All other ARCMT2 pedigrees with heterozygous haplotypes had a negative or borderline significant cumulative logarithm of odds score by the genetic program HOMOG (Ott, 1983).

We detected 15 different ALS5/SPG11/*KIAA1840* mutations in 29 affected individuals from 12 of 28 unrelated families with ARCMT2 (Table 1). Nine of these nucleotide changes were homozygous and six others, detected in the affected subjects of Families RM-801, RM-888 and CAM-006, were heterozygous compounds. All variants but one were truncating, including eight frameshift mutations, and six nonsense mutations. One nucleotide change (p.Arg945Gly) was a missense mutation. Variants segregated with the disease in all pedigrees and were absent in the panel of control chromosomes. Thirteen mutations had already been reported, while two (p.Gln198* and p.Pro2212Serfs*5) were novel and segregated with the disease (Table 1 and Fig. 2). Their pathogenic effect was predicted by bioinformatics analysis. In these families, the ALS5/SPG11/*KIAA1840* gene had no large deletions/duplications.

Genetic analysis of the other candidate genes (CMT2A2/HMSN2A2/*MFN2*, CMT2B1/*LMNA*, CMT2B2/*MED25*, CMT2B5/*NEFL*, ARCMT2F/dHMN2B/*HSPB1*, CMT2K/*GDAP1*, CMT2P/*LRSAM1*, CMT2R/*TRIM2*, CMT2S/*IGHMBP2*, CMT2T/*HSJ1*, CMTRID/*COX6A1*, ARAN-NM/*HINT*, GAN/*GAN*, SPG7/*PGN*, SPG15/*ZFYVE26*, SPG21/*ACP33*, SPG35/*FA2H*, SPG46/*GBA2*,

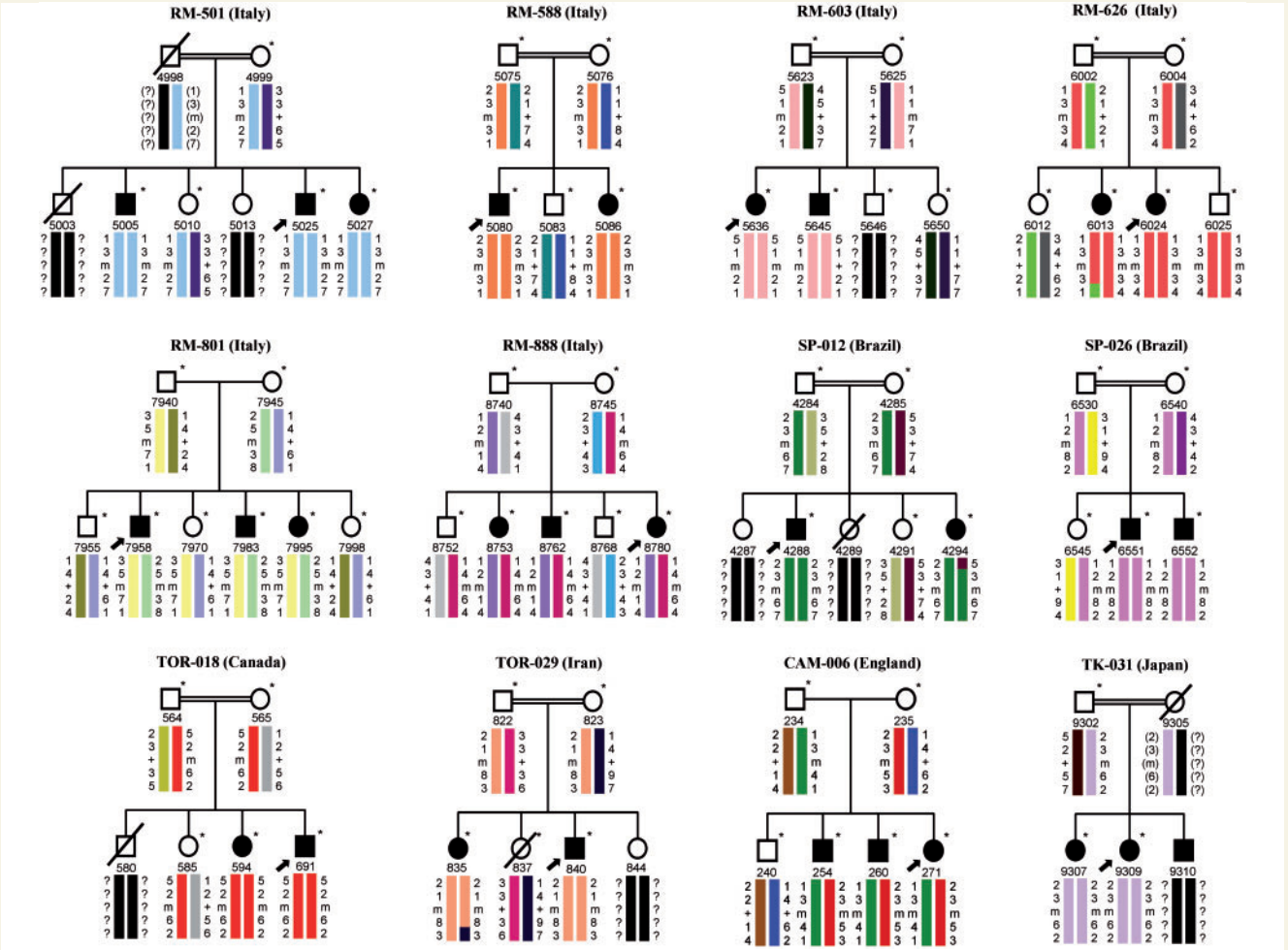

Figure 1 Pedigrees and segregation chart of 12 ARCMT2 families linked to the ALS5/SPG11 locus. Black solid symbols indicate affected individuals carrying ALS5/SPG11/*KIAA1840* mutations; white symbols represent unaffected subjects; square symbols are males, circles are females, and slashed symbols are deceased individuals. Individuals are reported as code numbers below the symbols. Probands are marked by arrows. Colour barcodes define the haplotypes created with markers D15S146, D15S537, D15S659, and D15S123, from *top* to *bottom*. Reconstructed genotypes are indicated by parentheses and question marks symbolize alleles that could not be reconstructed. The ALS5/SPG11/*KIAA1840* gene is placed between markers D15S537 and D15S659; key recombination events are observed between markers D15S659 and D15S123 in Patients 6013 (Family RM-626) and 835 (Family TOR-029), as well as between markers D15S146 and D15S537 in Patient 4294 (Family SP-012). * = sample subjects; m = mutation; + = wild-type.

SPG56/*CYP2U1*, and *SLC12A6*) did not reveal any coding mutations in the unrelated 28 families with ARCMT2. Direct sequencing of *POLG* and *TYMP* genes excluded mitochondrial disorders related to CMT2. Linkage analysis showed no linkage to chromosome 8q13-21.1 in all families (cumulative logarithm of odds score was −2.11 for marker D15S537 at $\theta = 0.0$).

Clinical findings of the ALS5/SPG11/*KIAA1840*-related ARCMT2 families

Among the 12 ALS5/SPG11/*KIAA1840* mutated pedigrees, nine showed consanguinity marriage (first-degree cousins) in their parents. Six families were from Italy, two from Brazil, one from England, and one from Japan. Moreover, two families were from Canada, one of which was an Iranian family who emigrated to Ontario (Fig. 1).

Affected subjects had a mainly distal, slowly progressive sensory and motor axonal neuropathy. The age at onset of the first motor symptoms in the 29 mutated ALS5/SPG11/*KIAA1840* patients oscillated from 4 to 35, with a mean of 11.4 ± 5.9 years. The mean age at examination was 25.1 ± 7.8 years (range 9–52).

A wide variation of phenotypic expression was detected (Table 2). Asymmetrical onset in lower limbs was present in 12 patients. Distal lower limb weakness was found in all affected individuals; 16 patients showed muscular weakness in upper limbs too. Wasting was frequent in lower limb muscles distally (69%) and in intrinsic hand muscles (48%). Lower limb fasciculations were detected in eight patients. No patient showed pontobulbar signs, such as

Table 1 Mutations identified in the ALS5/SPG11/*KIAA1840* gene

Family	Location	Mutation (cDNA)	Effect on protein	RFLP	Neuropathy[a]	Reference study
RM-501	Exon 2	c.398delG	p.Cys133Leufs*22	SfcI (loss)	SM	Paisan-Ruiz *et al.*, 2008
RM-588	Exon 15	c.2678G>A	p.Trp893*	–	M	Bettencourt *et al.*, 2014
RM-603	Exon 4	c.704_705delAT	p.His235Argfs*12	BsiI (gain)	SM	Stevanin *et al.*, 2007*b*
RM-626	Exon 1	c.118C>T	p.Gln40*	–	SM	Stevanin *et al.*, 2007*a*
RM-801	Exon 3	c.592C>T	p.Gln198*	BsgI (loss)	–	This study
	Exon 3	c.529_533delATATT	p.Ile177Serfs*2	AseI[b] (loss)	SM	Stevanin *et al.*, 2007*a*
RM-888	Exon 36	c.6632dupG	p.Pro2212fs*5	Cfr10I (gain)	–	This study
	Exon 32	c.6100C>T	p.Arg2034*	Cac8I[b] (loss)	M/SM[c]	Stevanin *et al.*, 2007*a*
SP-012	Exon 37	c.6832_6833delAG	p.Ser2278Leufs*61	–	M	Stevanin *et al.*, 2007*b*
SP-026	Exon 38	c.6856C>T	p.Arg2286*	MaeIII (gain)	SM	Denora *et al.*, 2009
TOR-018	Exon 15	c.2697G>A	p.Trp899*	–	SM	Denora *et al.*, 2009
TOR-029	Exon 15	c.2833A>G	p.Arg945Gly	MscI (loss)	SM	Stevanin *et al.*, 2007*b*
CAM-006	Exon 7	c.1549_1550delCT	p.Leu518Leufs*39	AhdI (gain)	SM	Stevanin *et al.*, 2007*b*
	Exon 36	c.6739_6742delGAGT	p.Glu2247Leufs*14	TfiI (gain)	SM	Stevanin *et al.*, 2007*b*
TK-031	Exon 1	c.165del19	p.Ser56Alafs*7	Cac8I (loss)	SM	Pensato *et al.*, 2014

Gene nucleotide numbering was based on the reference sequence NM_025137.3, with the A of the ATG start codon as position 1.
del = deletion; fs = frameshift; ins = insertion; M = motor; SM = sensorimotor; RFLP = restriction fragment length polymorphism.
[a]Axonal peripheral neuropathy refers to previously reported features; [b]mismatch primer used; [c]axonal and demyelinating peripheral neuropathy.

jaw spasticity, poor palatal elevation, increased facial reflexes, masseter, pterygoids, sternocleidomastoid, tongue muscle weakness, or muscle atrophy with fasciculations. Four patients had proximal lower limb weakness. Loss of pinprick and light touch sensation was common and involved lower limbs in most cases (86%).

The most frequent additional signs were foot deformities (79%), mainly *pes cavus* and kyphoscoliosis (59%). Hand deformities were present in seven patients with longer disease duration. Ankle contracture was present in 14 patients (48%) and tremor in 10 (34%). Bladder disturbances and sexual dysfunctions were detected in about one-third of the affected subjects. Babinski's sign was present bilaterally in two unrelated patients. No affected subject showed cerebellar signs or retinal disease.

Brain MRI images were available for all mutated *KIAA1840* patients. Thin corpus callosum was evident in the three affected siblings of Family RM-801, with severe thinning of the anterior portion and mild thinning of the splenium (Fig. 3A). These patients had low scores in the Wechsler Intelligence Scales for Children IV Intelligence Quotient (ID 7958: 51, ID 7983: 49, and ID 7995: 62; at 13, 11, and 9 years, respectively) with poor school performance and deficit in memory and calculation tests. Normal corpus callosum and no mental retardation or cognitive deficits were observed in the other ARCMT2 *KIAA1840*-mutated subjects.

Haematological and biochemical profiles, including serum creatine kinase, were unremarkable in all subjects. Lysosomal enzyme assay of peripheral blood leucocytes revealed that both β-hexosaminidase A and B isoenzymes were present at normal levels. Vitamins were within normal range. The CSF analysis was within normal range in the five patients analysed.

The disease was slowly progressive and most patients (86%) expressed mild-to-moderate phenotypes (Charcot–Marie–Tooth neuropathy score < 20); only two patients, one of which was wheelchair bound, reached Functional Disability Scale scores > 5 (Table 2).

Motor and sensory conduction studies showed motor and sensory axonal neuropathy, more prominent in lower limbs, with low amplitudes of compound motor and sensory nerve action potentials. Motor and sensory nerve conduction velocities were normal or slightly reduced, according to the secondary demyelinating processes. All motor nerve conduction velocities of median nerves were >38 m/s, differentiating CMT2 from CMT1. In 29 affected individuals, EMG of the tibialis anterior muscle detected predominant findings of chronic denervation/reinnervation (motor unit action potentials with long duration and large amplitude, or polyphasic, along with single or mixed interference patterns), and/or active denervation signs (fibrillation potentials, positive sharp waves, as well as fasciculation potentials). In 11 affected subjects, EMG of the abductor pollicis brevis muscle showed similar neurophysiological characteristics (Table 3).

Neuropathological analyses of the sural nerve biopsies were performed in 17 mutated patients and showed loss of myelinated fibres (Fig. 4A), mainly in fibres of large calibre, in line with the diagnosis of CMT2.

See the online Supplementary material for indicative case reports of patients with novel ALS5/SPG11/*KIAA1840* mutations.

Discussion

The ALS5/SPG11/*KIAA1840* gene was analysed in ARCMT2 patients from 28 unrelated pedigrees and a high frequency of pathogenic mutations, two of which were novel, was found in 12 families (43%), appearing to be a significant cause of ARCMT2. Our study showed

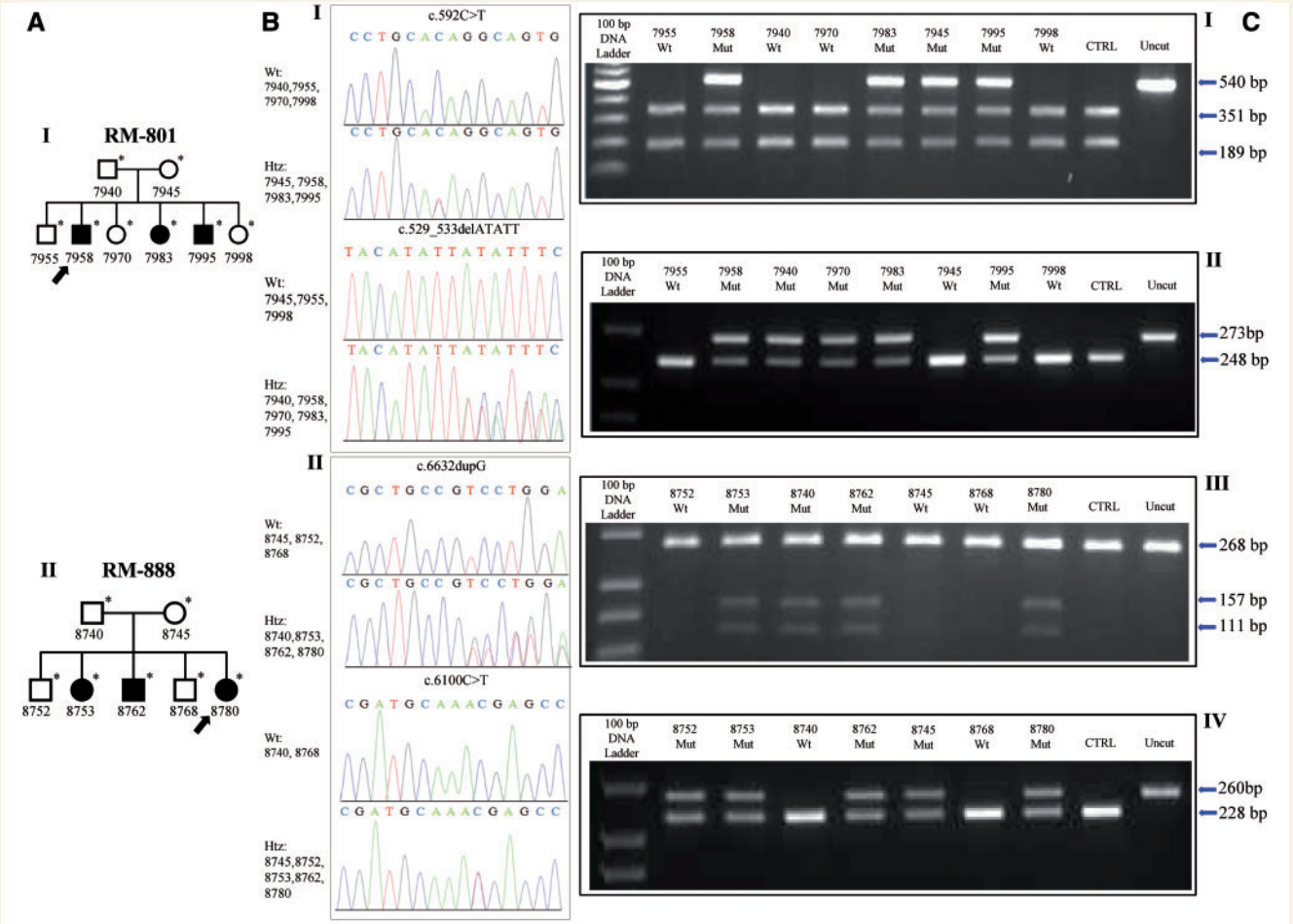

Figure 2 Pedigree charts, electropherograms and PCR-restriction fragment length polymorphism assays of families with novel ALS5/SPG11/*KIAA1840* mutations. (**A**) Pedigree charts RM-801 (**I**) and RM-888 (**II**). (**B**) Electropherogram of exon 3 of the ALS5/SPG11/*KIAA1840* gene in individuals of Family RM-801 (**I**), showing compound heterozygous status in the affected subjects (ID 7958, ID 7983, and ID 7995), as well as heterozygous status in the relatives (ID 7940, ID 7945, and ID 7970). (**II**) Electropherogram of exon 36 and exon 32 of the ALS5/SPG11/*KIAA1840* gene in individuals of Family RM-888 (**II**), displaying compound heterozygous status in the affected subjects (ID 8753, ID 8762, and ID 8780), and heterozygous status in the relatives (ID 8740, ID 8745, and ID 8752). (**C**) PCR-restriction fragment length polymorphism assays. After BsgI digestion, heterozygous individuals of Family RM-801 show three bands at 540, 351, and 189 base pairs (bp), while wild-type subjects display two bands at 351 and 189 bp (**I**). AseI digestion proves one band in wild-type components at 248 bp, as well as two bands at 273 and 248 bp in mutated individuals (**II**). *Cfr*10I digestion (c.6632dupG) leads to three bands at 268, 157, and 111 bp in heterozygous samples and one band at 268 bp (uncleaved) in wild-type components of Family RM-888 (**III**). Assay with enzyme Cac8I displays one band in wild-type individuals at 228 bp, as well as two bands at 260 and 228 bp in mutated subjects (**IV**). Wt = wild-type; Htz = heterozygous; Mut = mutated.

novel genotype–phenotype correlation, which further broadens the clinical spectrum associated with ALS5/SPG11/*KIAA1840* mutations (Fig. 5). Therefore, genetic screening of the ALS5/SPG11/*KIAA1840* gene should be considered not only in patients with ARHSP with thin corpus callosum and in affected individuals with ARJALS, but also in affected subjects with ARCMT2. Due to the complexity and heterogeneity of these neurodegenerative diseases, next-generation sequencing techniques are the most effective diagnostic tool to identify the genetic cause in patients with myelopathy or neuropathy, either by targeted sequencing panel approach or by whole-genome sequencing.

This clinical–genetic entity shows a worldwide distribution, since the pedigrees carrying mutations in ALS5/SPG11/*KIAA1840* were from Italy, Brazil, Canada, England, Iran, and Japan. The variants are scattered throughout the entire amino acid sequence, without evidence of 'hot spots', and 93% were truncating mutations. This finding is consistent with previous studies describing mostly mutations leading to the truncation of the ALS5/SPG11 protein and consequent loss of function mechanism (Pensato *et al.*, 2014). Furthermore, a probable mechanism of nonsense-mediated mRNA decay might also be hypothesized (Paisan-Ruiz *et al.*, 2008).

The two unrelated ARCMT2 patients with bilateral Babinski's sign further enlarge the clinical spectrum of the disorder, showing that *KIAA1840*-related diseases might be clinically suspected if neuropathy is present in addition to

Table 2 Clinical features of 29 patients with ALS5/SPG11/*KIAA1840* mutations

Onset[a] in the second decade of life	21 (72)
Disease duration >10 years	18 (62)
Males	15 (52)
Females	14 (48)
Muscle weakness	
Distal lower limbs	29 (100)
Proximal lower limbs	4 (14)
Distal upper limbs	16 (55)
Proximal upper limbs	0 (0)
Muscle wasting	
Distal lower limbs	20 (69)
Proximal lower limbs	1 (3)
Hands	14 (48)
Loss of pinprick and light touch in lower limbs	25 (86)
Loss of proprioception in lower limbs	15 (52)
Loss of pinprick and light touch in upper limbs	8 (28)
Loss of proprioception in upper limbs	0 (0)
Total absence of deep tendon reflexes	
Lower limbs	8 (28)
Upper limbs	2 (7)
Asymmetrical onset	12 (41)
Positive Romberg test	7 (24)
Gait impairment	18 (62)
Babinski sign	2 (7)
Postural tremor	10 (34)
Wrist contracture	3 (10)
Elbow contractures	1 (3)
Ankle contracture	14 (48)
Calf hypertrophy	4 (14)
Foot deformities	23 (79)
Fasciculations	
Lower limbs	8 (28)
Upper limbs	1 (3)
Foot drop	11 (38)
Hand deformities	7 (24)
Kyphoscoliosis	17 (59)
Mental retardation	3 (10)
Thin corpus callosum	3 (10)
Cerebellar signs	0 (0)
Retinal disease	0 (0)
Grey matter atrophy on brain MRI	1 (3)
White matter abnormalities on brain MRI	0 (0)
Bladder disturbances	9 (31)
Sexual dysfunctions	7 (24)
Spasticity	0 (0)
FDS 0-2	14 (48)
FDS 3-5	13 (45)
FDS 6-8	2 (7)*
CMTNS mild	9 (31)
CMTNS moderate	16 (55)
CMTNS severe	4 (14)#

Values are *n* (%).

[a]Age at onset was calculated as the time when motor symptoms appeared. FDS (Functional Disability Scale) from 0 to 8 as follows: 0 = normal; 1 = normal, but with cramps and fatigability; 2 = inability to run; 3 = walking difficult, but still possible unaided; 4 = able to walk with a cane; 5 = able to walk with crutches; 6 = able to walk with a walker; 7 = wheelchair bound; 8 = bedridden. CMTNS = Charcot-Marie-Tooth Neuropathy Score: mild (⩽10), moderate (11–20), and severe (>20). *Ages at onset were 4 and 9 years; #ages at onset were 4, 8, 9, and 12 years.

upper motor neuron signs or symptoms, e.g. deep tendon reflexes are symmetrically diminished in the lower extremities with bilateral positive Babinski's sign. Moreover, the impairment of higher mental functions impairment and brain alterations at MRI in three affected siblings of one ARCMT2 family should be noted. Indeed, the presence of clinical signs of leukoencephalopathy, as well as white matter alterations at brain MRI, has been previously reported in demyelinating, axonal, and intermediate forms of the disorder (Genari *et al.*, 2011; Reyes-Marin *et al.*, 2011; Sagnelli *et al.*, 2014). Therefore, we believe that brain MRI and neuropsychological testing are useful tools in the clinical work-up of patients with Charcot–Marie–Tooth disease. To our knowledge, this is the first report of ALS5/SPG11/*KIAA1840* mutations in subjects with ARCMT2 and all of our families can be classified as CMT2X, according to the classification of the Charcot–Marie–Tooth disease currently used in OMIM (http://www.ncbi.nlm.nih.gov/omim).

The disease has a slow progression and affected subjects with earlier onset show a more severe phenotype compared to those with late onset. Overall, the age at onset is the second decade of life, in line with both ARCMT2 and ARHSP (Tazir *et al.*, 2013; Lo Giudice *et al.*, 2014). Clinical heterogeneity is well documented in ALS5/SPG11/*KIAA1840* mutations causing ARHSP, ranging from the most frequent association of thin corpus callosum, white matter alterations, mental retardation, cerebellar signs, and axonal peripheral neuropathy, to less common clinical findings, such as seizures, abnormal eye signs, maculopathy, amyotrophy, and parkinsonism (Tessa *et al.*, 2014). In addition, ALS5/SPG11/*KIAA1840* mutations have been often found in patients with ARJALS (Orlacchio *et al.*, 2010). Interestingly, no specific differences in the type of variants, or position within the primary amino acid sequence, were observed. Even identical mutations causing different phenotypes were found (Fig. 5), confirming that variants at the same locus can lead to distinct phenotypes (Hegele, 2005). This aspect is not uncommon in monogenic diseases and demonstrates how genotype–phenotype associations can be often unpredictable.

The complexity of a correct clinical classification of motor neuron diseases linked to spatacsin is further increased by the presence of ALS5/SPG11/*KIAA1840* mutations in patients with an overlapping phenotype, exhibiting features of amyotrophic lateral sclerosis as well as spastic paraplegia, as described by Querin *et al.* (2014).

As previously hypothesized, the ALS5/SPG11/*KIAA1840* phenotype results from the combined degeneration of central and peripheral axons (Hehr *et al.*, 2007). In particular, peripheral neuropathy might affect both sensory and motor fibres and might lead to pure distal amyotrophy, as well as to CMT2. The roles of spatacsin in the cellular pathway of axonal maintenance, including cargo trafficking, is becoming clearer: it is located in axons and dendrites, co-localized with cytoskeletal and synaptic vesicles, and it is present in synaptosomes (Chiurchiù *et al.*, 2014; Pérez-Brangulí *et al.*,

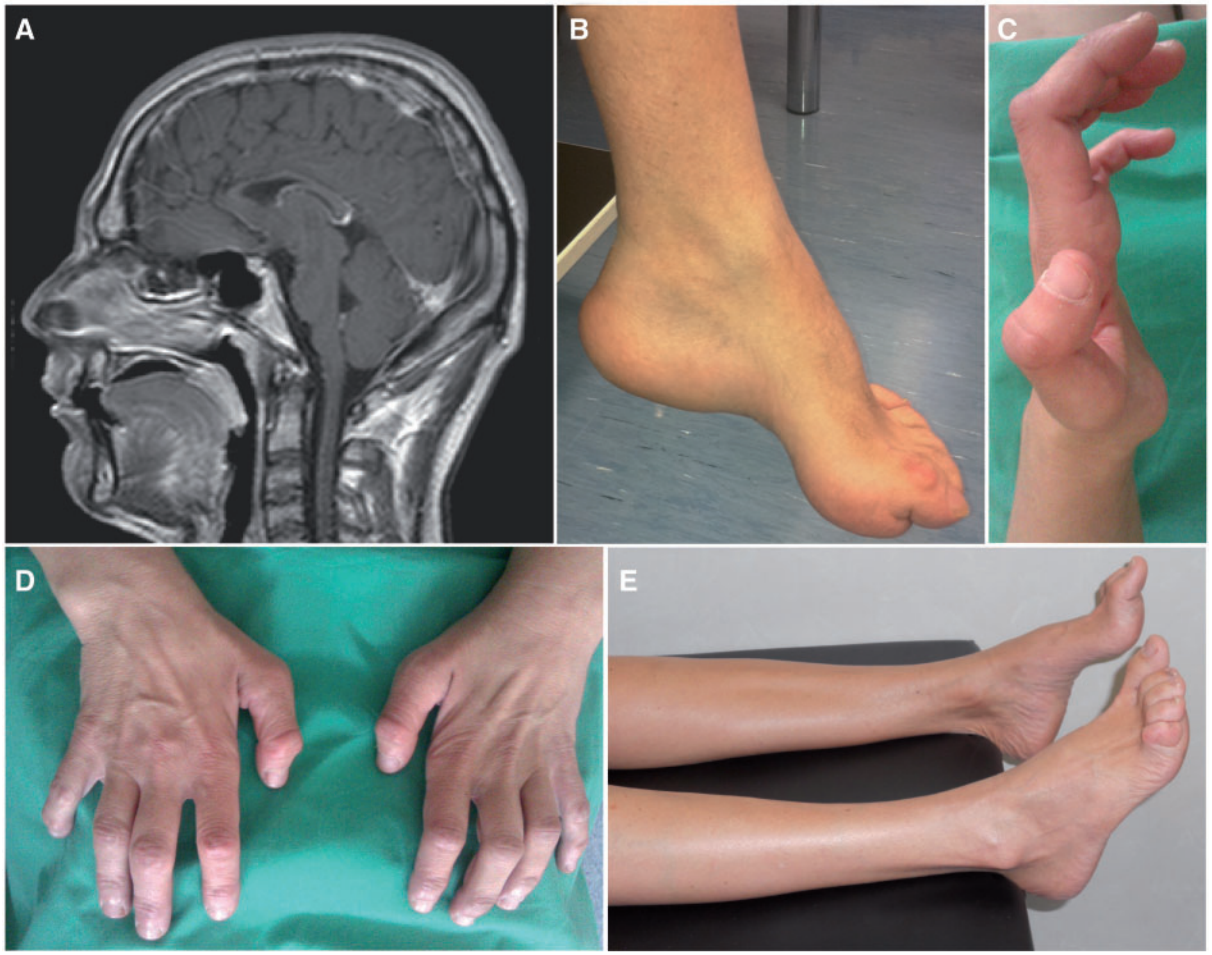

Figure 3 Clinical features of Patients 7958 (Family RM-801) and 8780 (Family RM-888). (**A**) T_1-weighted MRI showing thin corpus callosum in the proband of Family RM-801. (**B**) *Pes cavovarus* of the same patient. (**C**) Deformities and (**D**) global atrophy of hands in the proband of Family RM-888. (**E**) Atrophied legs with *pes cavus* of the same patient.

Table 3 Electroneurography and EMG characteristics in the 29 ALS5/SPG11/*KIAA1840*–mutated individuals

	Mean ± SD	Range	Reference lower value[a]	UR (subjects)	Pathological (subjects)[b]	Chronic denervation	Active denervation
Median nerve							
CMAP (mV)	3.6 ± 2.4	0.1–9.2	5	5	15	–	–
SNAP (μV)[c]	6.8 ± 5.3	0.4–21.7	9	6	16	–	–
MNCV (m/s)	48.1 ± 7.5	39–67	50	–	12	–	–
SNCV (m/s)	51.1 ± 8.2	35–64	54	–	13	–	–
Peroneal nerve							
CMAP (mV)	2.1 ± 3.8	0.1–11.8	3	13	26	–	–
MNCV (m/s)	38.3 ± 5.1	31–44	42	–	20	–	–
Tibial nerve							
CMAP (mV)	2.4 ± 3.9	0.1–16.5	4	14	27	–	–
MNCV (m/s)	38.1 ± 4.8	32–46	42	–	21	–	–
Sural nerve							
SNAP (μV)	2.3 ± 1.5	0.3–3.8	*	16	29	–	–
SNCV (m/s)	37.3 ± 5.2	31–47	42	–	22	–	–
TA muscle	–	–	–	–	29	23	8
APB muscle	–	–	–	–	11	9	3

APB = abductor pollicis brevis; CMAP = compound nervous motor action potential (amplitude); MNCV = motor nerve conduction velocity; SD = standard deviation; SNAP = sensory nerve action potential (amplitude); SNCV = sensory nerve conduction velocity; TA = tibialis anterior; UR = unrecordable (action potentials). [a]Reference lower value is the lower limit assessed by our laboratories; [b]The 'Pathological' column includes non–recordable items; [c]Orthodromic evaluation. *SNAP reference lower value of sural nerve is calculated as: 11.34 − (0.092 × age in years) − 5.04 μV (Bienfait, 2007).

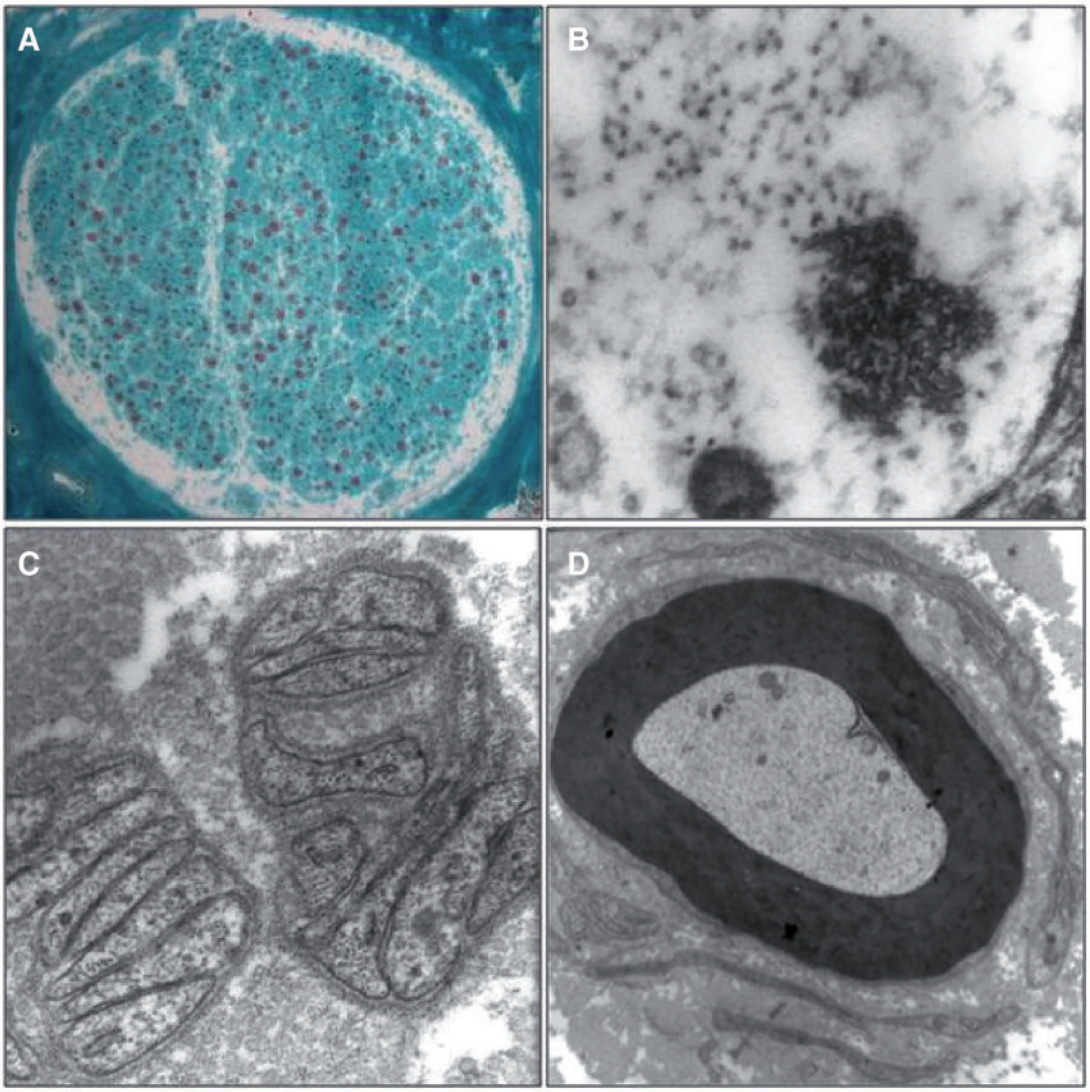

Figure 4 Sural nerve biopsy of Patient 7958 (Family RM-801). (**A**) Transverse cryostat section showing a nerve fascicle with medium grade myelinated fibre loss. Modified Gomori Trichrome Stain, ×80. (**B–D**) Transmission electron micrographs showing: (**B**) an unmyelinated fibre displaying intra-axonal aggregates, seemingly composed by neurotubules and neurofilaments, ×85 000; (**C**) flattened Schwann cell processes indicating unmyelinated axon loss, ×30 000; (**D**) a rudimentary onion bulb surrounding an apparently intact myelinated fibre, possibly indicating secondary Schwann cell pathology, ×7000.

2014). Other forms of hereditary spastic paraplegia linked to proteins involved in axon maintenance, such as kinesin SPG10/*KIF5A* and SPG17/*BSCL2*, are known to be allelic to CMT2 (Goizet *et al.*, 2009; Ito and Suzuki, 2009; Crimella *et al.*, 2012; Timmerman *et al.*, 2013). Furthermore, mutations in SPG4/*SPAST*, SPG3A/*ATL1*, SPG17/*BSCL2*, as well as SPG43/*C19orf12* might cause spastic paraplegia and axonal peripheral neuropathy with atrophy of small hand muscles (Silver syndrome) (Windpassinger *et al.*, 2004; Orlacchio *et al.*, 2008; Fusco *et al.*, 2010; Landouré *et al.*, 2013). Besides, mutations in *ATL1*, whose protein is implicated in neurite outgrowth, intracellular membrane trafficking, and axon elongation during neuronal development (Byrnes and Sondermann, 2011), might cause hereditary sensory neuropathy type I (HSN-I) with or without pyramidal tract features (Guelly *et al.*, 2011; Leonardis *et al.*, 2012).

Remarkably, the previously reported mutations in ALS5/SPG11/*KIAA1840* were often associated with ARHSP complicated by axonal peripheral neuropathy, mainly motor, but also sensory (Table 1). In *KIAA1840* mutations, a preferential involvement of the CNS or the peripheral nervous system may be due to different causes. First of all, the blood–nerve barrier might influence protein expression in peripheral axons, as well as the blood–brain barrier in central axons. Moreover, ALS5/SPG11/*KIAA1840* knockdown in Zebrafish (*Danio rerio*) reveals a compromised outgrowth of spinal motor axons, thus indicating that

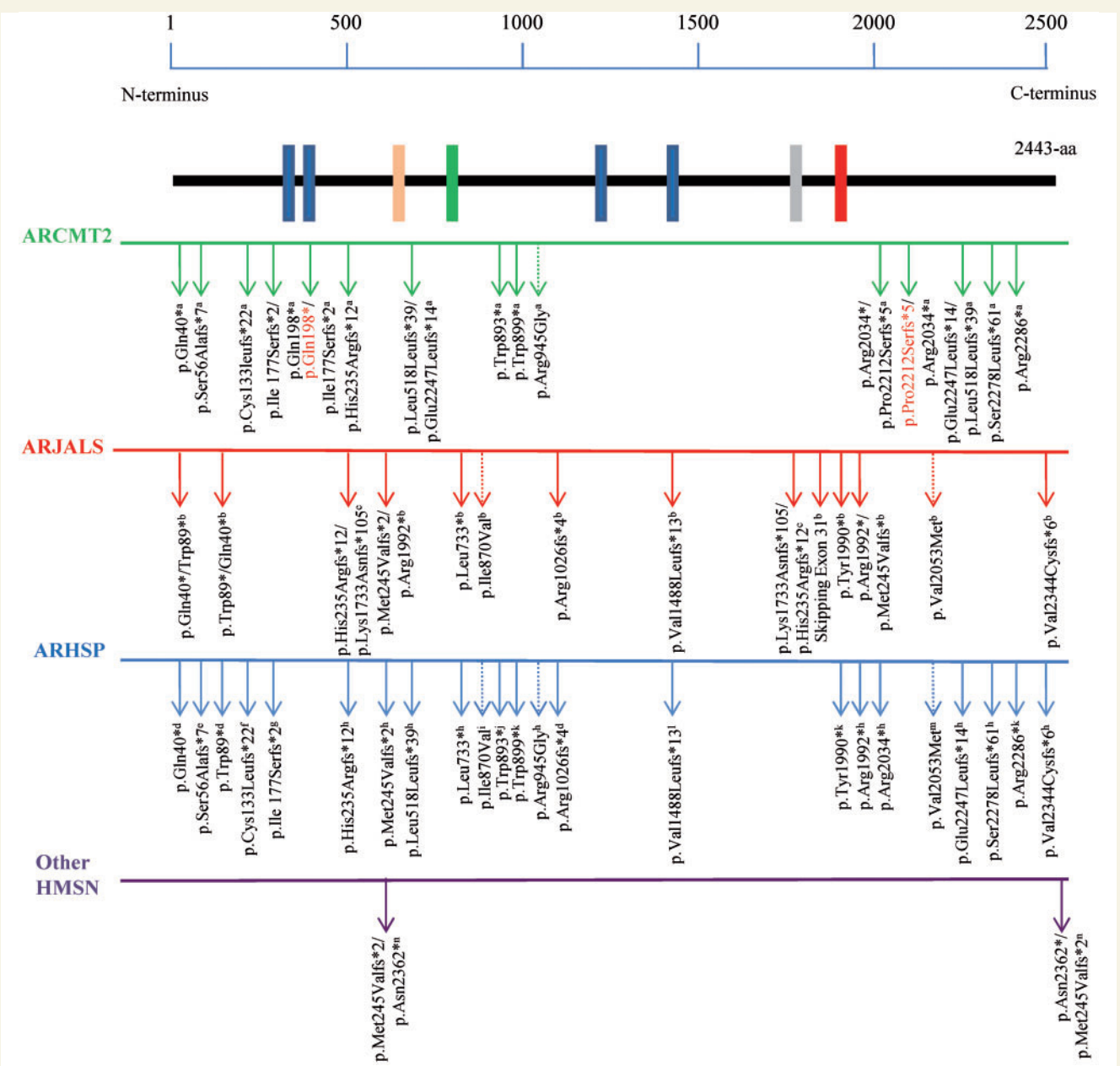

Figure 5 Schematic representation of the ALS5/SPG11 protein and position of previously reported (black) and novel (red) mutations, stratified by distinctive phenotypes. Specific mutations for clinical heterogeneity are represented. Putative functional domains are depicted as rectangles, and their positions within the amino acid sequence are indicated: the transmembrane domain (blue box; positions, 163–194, 200–240, 1239–1267, and 1471–1493), glycosyl hydroxylase F1 signature (pink box; position, 482–490), leucine zipper (green box; position, 611–632), coil-coil domain (grey box; position, 1556–1590), and Myb domain (red box; position 1766–1774). Arrows indicate truncating mutations; dotted arrows indicate missense mutations. Aa = amino acids. [a]This study; [b]Orlacchio *et al.*, 2010; [c]Daoud *et al.*, 2012; [d]Hehr *et al.*, 2007; [e]Pensato *et al.*, 2014; [f]Paisan-Ruiz *et al.*, 2008; [g]Stevanin *et al.*, 2007*a*; [h]Stevanin *et al.*, 2007*b*; [i]Pippucci *et al.*, 2009; [j]Bettencourt *et al.*, 2014; [k]Denora *et al.*, 2009; [l]Lee *et al.*, 2008; [m]Del Bo *et al.*, 2007; [n]Querin *et al.*, 2014.

spatacsin is involved in the formation of neuromuscular junctions during development (Martin *et al.*, 2012). The association in synaptosomes of spatacsin with spastizin (SPG15/*ZFYVE26*) and with the adaptor protein complex 5 (SPG48/*KIAA0415*) (Hirst *et al.*, 2013) suggests that the loss of function of spatacsin could not be the only mechanism for axonal dysfunction in ALS5/SPG11/*KIAA1840*-mutated patients. Indeed, it may be hypothesized that a variable phenotypic expression of *KIAA1840* mutations results from the interaction of gene modifier factors. Further studies are necessary to clarify whether allelic heterogeneity depends on environmental or other genetic/epigenetic factors. In conclusion, the presence of common molecular, pathological, and genetic features in *KIAA1840*-related

diseases, suggests that the different phenotypes of axonal degeneration induced by ALS5/SPG11/*KIAA1840* mutations may be targeted by common therapeutic strategies.

Acknowledgements

We thank the patients and their family members for taking part in this study. We thank Michela Renna (MA) for her language advice and assistance, Martina Di Lullo (BSc) and Valerio Battisti (BSc) for the technical support, and the members of our laboratories for the stimulating discussions and helpful comments on this manuscript. We are extremely grateful to the *Genetic Bank* of the *Laboratorio di Neurogenetica, CERC - IRCCS Santa Lucia*, Rome, Italy (http://www.hsantalucia.it/neurogen/index_en.htm) for the service provided.

Funding

This work was supported by the Italian *Ministero della Salute* (Grant no. GR09.109 to A.O.), the *Comitato Telethon Fondazione Onlus*, Italy (Grant no. GGP10121 to A.O.), the *Università di Roma* "*Tor Vergata*", Rome, Italy (Grant no. E82I15000190005 to A.O.), the *Rotary Club Sanluri Medio Campidano*, Sanluri (VS), Italy (Grant *Noi per Voi* to A.O.), the Japan Society for the Promotion of Science (JSPS KAKENHI Grant no. 26461294 to T.K.), the Ministry of Health, Labour, and Welfare of Japan (Grant for research on rare and intractable diseases and establishment of novel treatments for amyotrophic lateral sclerosis to T.K.), and the Brain Science Foundation, Japan (Grant to T.K.).

Supplementary material

Supplementary material is available at *Brain* online.

References

American Psychiatric Association. Diagnotic and statistical manual of mental disorders. 5th edn. Arlington, VA: American Psychiatric Association; 2013. http://dx.doi.org/10.1176/appi.books.9780890425596

Barhoumi C, Amouri R, Ben Hamida C, Ben Hamida M, Machghoul S, Gueddiche M, et al. Linkage of a new locus for autosomal recessive axonal form of Charcot-Marie-Tooth disease to chromosome 8q21.3. Neuromuscul Disord 2001; 11: 27–34.

Bettencourt C, López-Sendón JL, García-Caldentey J, Rizzu P, Bakker IM, Shomroni O, et al. Exome sequencing is a useful diagnostic tool for complicated forms of hereditary spastic paraplegia. Clin Genet 2014; 85: 154–8.

Bienfait HME. Axonal phenotypes in Charcot-Marie-Tooth disease. Amsterdam, The Netherlands: Faculty of Medicine, University of Amsterdam (AMC-UvA); 2007. http://dare.uva.nl/document/2/47043

Bird DT. GeneReviews [Internet] In: Pagon RA, Adam MP, Ardinger HH, Bird DT, Dolan CR, Fong CT, et al., editors. Charcot-Marie-Tooth neuropathy type 2. Seattle, WA: University of Washington, Seattle; 1993-2015. http://www.ncbi.nlm.nih.gov/books/NBK1285/

Birouk N, Gouider R, Le Guern E, Gugenheim M, Tardieu S, Maisonobe T, et al. Charcot-Marie-Tooth disease type 1A with 17p11.2 duplication. Clinical and electrophysiological phenotype study and factors influencing disease severity in 119 cases. Brain 1997; 120: 813–23.

Bomont P, Cavalier L, Blondeau F, Ben Hamida C, Belal S, Tazir M, et al. The gene encoding gigaxonin, a new member of the cytoskeletal BTB/kelch repeat family, is mutated in giant axonal neuropathy. Nat Genet 2000; 26: 370–4.

Byrnes LJ, Sondermann H. Structural basis for the nucleotide-dependent dimerization of the large G protein atlastin-1/SPG3A. Proc Natl Acad Sci USA 2011; 108: 2216–21.

Carlesimo GA, Caltagirone C, Gainotti G. The mental deterioration battery: normative data, diagnostic reliability and qualitative analyses of cognitive impairment. The group for the standardization of the mental deterioration battery. Eur Neurol 1996; 36: 378–84.

Carosi L, Lo Giudice T, Di Lullo M, Lombardi F, Babalini C, Gaudiello F, et al. Hereditary spastic paraplegia: a novel mutation and expansion of the phenotype variability in SPG10. J Neurol Neurosurg Psychiatry 2015; 86: 702–4.

Casari G, De Fusco M, Ciarmatori S, Zeviani M, Mora M, Fernandez P, et al. Spastic paraplegia and OXPHOS impairment caused by mutations in paraplegin, a nuclear-encoded mitochondrial metalloprotease. Cell 1998; 93: 973–83.

Cassereau J, Codron P, Funalot B. Inherited peripheral neuropathies due to mitochondrial disorders. Rev Neurol (Paris) 2014; 170: 366–74.

Chiurchiù V, Maccarrone M, Orlacchio A. The role of reticulons in neurodegenerative diseases. Neuromolecular Med [Review] 2014; 16: 3–15.

Claramunt R, Pedrola L, Sevilla T, López de Munain A, Berciano J, Cuesta A, et al. Genetics of Charcot-Marie-Tooth disease type 4A: mutations, inheritance, phenotypic variability, and founder effect. J Med Genet 2005; 42: 358–65.

Cottenie E, Kochanski A, Jordanova A, Bansagi B, Zimon M, Horga A, et al. Truncating and missense mutations in *IGHMBP2* cause Charcot-Marie Tooth disease type 2. Am J Hum Genet 2014; 95: 590–601.

Crimella C, Baschirotto C, Arnoldi A, Tonelli A, Tenderini E, Airoldi G, et al. Mutations in the motor and stalk domains of *KIF5A* in spastic paraplegia type 10 and in axonal Charcot-Marie-Tooth type 2. Clin Genet 2012; 82: 157–64.

Daoud H, Zhou S, Noreau A, Sabbagh M, Belzil V, Dionne-Laporte A, et al. Exome sequencing reveals SPG11 mutations causing juvenile ALS. Neurobiol Aging 2012; 33: 839. e5–9.

De Sandre-Giovannoli A, Chaouch M, Kozlov S, Vallat JM, Tazir M, Kassouri N, et al. Homozygous defects in *LMNA*, encoding lamin A/C nuclear-envelope proteins, cause autosomal recessive axonal neuropathy in human (Charcot-Marie-Tooth disorder type 2) and mouse. Am J Hum Genet 2002; 70: 726–36.

Del Bo R, Di Fonzo A, Ghezzi S, Locatelli F, Stevanin G, Costa A, et al. SPG11: a consistent clinical phenotype in a family with homozygous spatacsin truncating mutation. Neurogenetics 2007; 8: 301–5.

Denora PS, Schlesinger D, Casali C, Kok F, Tessa A, Boukhris A, et al. Screening of ARHSP-TCC patients expands the spectrum of SPG11 mutations and includes a large scale gene deletion. Hum Mutat 2009; 30: 500–19.

Dyck PJ, Thomas PK, editors. Peripheal neuropathy. 4th edn. Philadelphia, PA: Elsevier Saunders; 2005. http://www.scribd.com/doc/243563627/Peripheral-Neuropathy-2005-Dyck-pdf#scribd

Dyck PJ, Gutrecht JA, Bastron JA, Karnes WE, Dale AJ. Histologic and teased-fiber measurements of sural nerve in disorders of lower motor and primary sensory neurons. Mayo Clin Proc 1968; 43: 81–123.

Feely S, Laura M, Siskind CE, Sottile S, Davis M, Gibbons VS, et al. *MFN2* mutations cause severe phenotypes in most patients with CMT2A. Neurology 2011; 76:1690–6.

Fridman V, Murphy SM. The spectrum of axonopathies: from CMT2 to HSP. Neurology 2014; 83: 580–1.

Fusco C, Frattini D, Farnetti E, Nicoli D, Casali B, Fiorentino F, et al. Hereditary spastic paraplegia and axonal motor neuropathy caused by a novel SPG3A *de novo* mutation. Brain Dev 2010; 32: 592–4.

Genari AB, Borghetti VH, Gouvêa SP, Bueno KC, dos Santos PL, dos Santos AC, et al. Characterizing the phenotypic manifestations of *MFN2* R104W mutation in Charcot-Marie-Tooth type 2. Neuromuscul Disord 2011; 21: 428–32.

Gess B, Auer-Grumbach M, Schirmacher A, Strom T, Zitzelsberger M, Rudnik-Schöneborn S, et al. *HSJ1*-related hereditary neuropathies: novel mutations and extended clinical spectrum. Neurology 2014; 83: 1726–32.

Goizet C, Boukhris A, Mundwiller E, Tallaksen C, Forlani S, Toutain A, et al. Complicated forms of autosomal dominant hereditary spastic paraplegia are frequent in SPG10. Hum Mutat 2009; 30: 376–85.

Guelly C, Zhu PP, Leonardis L, Papić L, Zidar J, Schabhüttl M, et al. Targeted high-throughput sequencing identifies mutations in atlastin-1 as a cause of hereditary sensory neuropathy type I. Am J Hum Genet 2011; 88: 99–105.

Guernsey DL, Jiang H, Bedard K, Evans SC, Ferguson M, Matsuoka M, et al. Mutation in the gene encoding ubiquitin ligase LRSAM1 in patients with Charcot-Marie-Tooth disease. PLoS Genet 2010; 6: e1001081.

Hammer MB, Eleuch-Fayache G, Schottlaender LV, Nehdi H, Gibbs JR, Arepalli SK, et al. Mutations in *GBA2* cause autosomal-recessive cerebellar ataxia with spasticity. Am J Hum Genet 2013; 92: 245–51.

Hanein S, Martin E, Boukhris A, Byrne P, Goizet C, Hamri A, et al. Identification of the SPG15 gene, encoding spastizin, as a frequent cause of complicated autosomal-recessive spastic paraplegia, including Kjellin syndrome. Am J Hum Genet 2008; 82: 992–1002.

Hegele R. *LMNA* mutation position predicts organ system involvement in laminopathies. Clin Genet 2005; 68: 31–4.

Hehr U, Bauer P, Winner B, Schüle R, Olmez A, Koehler W, et al. Long-term course and mutational spectrum of spatacsin-linked spastic paraplegia. Ann Neurol 2007; 62: 656–65.

Hirst J, Borner GH, Edgar J, Hein MY, Mann M, Buchholz F, et al. Interaction between AP-5 and the hereditary spastic paraplegia proteins SPG11and SPG15. Mol Biol Cell 2013; 24: 2558–69.

Houlden H, Laura M, Wavrant-De Vrièze F, Blake J, Wood N, Reilly MM. Mutations in the *HSP27* (*HSPB1*) gene cause dominant, recessive, and sporadic distal HMN/CMT type 2. Neurology 2008; 71: 1660–8.

Howard HC, Mount DB, Rochefort D, Byun N, Dupré N, Lu J, et al. The K-Cl cotransporter KCC3 is mutant in a severe peripheral neuropathy associated with agenesis of the corpus callosum. Nat Genet 2002; 32: 384–92. Erratum in Nat Genet 2002; 32: 681.

Ito D, Suzuki N. Seipinopathy: a novel endoplasmic reticulum stress-associated disease [Review]. Brain 2009; 132: 8–15.

Jerath NU, Shy ME. Hereditary motor and sensory neuropathies: Understanding molecular pathogenesis could lead to future treatment strategies. Biochim Biophys Acta 2015; 1852: 667–78.

Landouré G, Zhu PP, Lourenço CM, Johnson JO, Toro C, Bricceno KV, et al. Hereditary spastic paraplegia type 43 (SPG43) is caused by mutation in *C19orf12*. Hum Mutat 2013; 34: 1357–60.

Leal A, Huehne K, Bauer F, Sticht H, Berger P, Suter U, et al. Identification of the variant Ala335Val of *MED25* as responsible for CMT2B2: molecular data, functional studies of the SH3 recognition motif and correlation between wild-type *MED25* and *PMP22* RNA levels in CMT1A animal models. Neurogenetics 2009; 10: 275–87.

Lee MJ, Cheng TW, Hua MS, Pan MK, Wang J, Stephenson DA, et al. Mutations of the SPG11 gene in patients with autosomal recessive spastic paraparesis and thin corpus callosum. J Neurol Neurosurg Psychiatry 2008; 79: 607–9.

Leonardis L, Auer-Grumbach M, Papić L, Zidar J. The N355K atlastin 1 mutation is associated with hereditary sensory neuropathy and pyramidal tract features. Eur J Neurol 2012; 19: 992–8.

Lo Giudice T, Lombardi F, Santorelli FM, Kawarai T, Orlacchio A. Hereditary spastic paraplegia: clinical-genetic characteristics and evolving molecular mechanisms [Review]. Exp Neurol 2014; 261: 518–39.

Martin E, Schüle R, Smets K, Rastetter A, Boukhris, A, Loureiro JL, et al. Loss of function of glucocerebrosidase *GBA2* is responsible for motor neuron defects in hereditary spastic paraplegia. Am J Hum Genet 2013; 92: 238–44.

Martin E, Yanicostas C, Rastetter A, Naini SM, Maouedj A, Kabashi E, et al. Spatacsin and spastizin act in the same pathway required for proper spinal motor neuron axon outgrowth in Zebrafish. Neurobiol Dis 2012; 48: 299–308.

Medical Research Council. Aids to the examination of the peripheral nervous system. Her Majesty's Stationery Office. London, UK; 1981, Memorandum no. 45.

Murphy SM, Herrmann DN, McDermott MP, Scherer SS, Shy ME, Reilly MM, et al. Reliability of the CMT neuropathy score (second version) in Charcot-Marie-Tooth disease. J Peripher Nerv Syst 2011; 16: 191–8.

Nicholson GA, Magdelaine C, Zhu D, Grew S, Ryan MM, Sturtz F, et al. Severe early-onset axonal neuropathy with homozygous and compound heterozygous *MFN2* mutations. Neurology 2008; 70: 1678–81.

Nishino I, Spinazzola A, Papadimitriou A, Hammans S, Steiner I, Hahn CD, et al. Mitochondrial neurogastrointestinal encephalomyopathy: an autosomal recessive disorder due to thymidine phosphorylase mutations. Ann Neurol 2000; 47: 792–800.

Orlacchio A, Patrono C, Gaudiello F, Rocchi C, Moschella V, Floris R, et al. Silver syndrome variant of hereditary spastic paraplegia: a locus to 4p and allelism with SPG4. Neurology 2008; 70: 1959–66.

Orlacchio A, Babalini C, Borreca A, Patrono C, Massa R, Basaran S, et al. Spatacsin mutations cause autosomal recessive juvenile amyotrophic lateral sclerosis. Brain 2010; 133: 591–8.

Ott J. Linkage analysis and family classification under heterogeneity. Ann Hum Genet 1983; 47: 311–20.

Palumbo C, Massa R, Panico MB, Di Muzio A, Sinibaldi P, Bernardi G, et al. Peripheral nerve extracellular matrix remodelling in Charcot-Marie-Tooth type I disease. Acta Neuropathol 2002; 104: 287–96.

Paisan-Ruiz C, Nath P, Wood NW, Singleton A, Houlden H. Clinical heterogeneity and genotype-phenotype correlations in hereditary spastic paraplegia because of spatacsin mutations (SPG11). Eur J Neurol 2008; 15: 1065–70.

Pehlivan D, Coban Akdemir Z, Karaca E, Bayram Y, Jhangiani S, Yildiz EP, et al. Exome sequencing reveals homozygous *TRIM2* mutation in a patient with early onset CMT and bilateral vocal cord paralysis. Hum Genet 2015; 134: 671–3.

Pensato V, Castellotti B, Gellera C, Pareyson D, Ciano C, Nanetti L, et al. Overlapping phenotypes in complex spastic paraplegias SPG11, SPG15, SPG35 and SPG48. Brain 2014; 137: 1907–20.

Pérez-Brangulí F, Mishra HK, Prots I, Havlicek S, Kohl Z, Saul D, et al. Dysfunction of spatacsin leads to axonal pathology in SPG11-linked hereditary spastic paraplegia. Hum Mol Genet 2014; 23: 4859–74.

Pierson TM, Simeonov DR, Sincan M, Adams DA, Markello T, Golas G, et al. Exome sequencing and SNP analysis detect novel compound heterozygosity in fatty acid hydroxylase-associated neurodegeneration. Eur J Hum Genet 2012; 20: 476–9.

Pippucci T, Panza E, Pompilii E, Donadio V, Borreca A, Babalini C, et al. Autosomal recessive hereditary spastic paraplegia with thin

corpus callosum: a novel mutation in the SPG11 gene and further evidence for genetic heterogeneity. Eur J Neurol 2009; 16: 121–6.

Querin G, Bertolin C, Martinuzzi A, Bassi MT, Arnoldi A, Polo A, et al. The blurred scenario of motor neuron disorders linked to spatacsin mutations: a case report. Eur J Neurol 2014; 21: 85–6.

Reyes-Marin K, Jimenez-Pancho J, Pozo L, Garcia-Villanueva M, de Blas G, Vazquez JM, Jimenez-Escrig A. A novel myelin protein zero (V136G) homozygous mutation causing late onset demyelinating polyneuropathy with brain white matter lesions. Clin Neurol Neurosurg 2011; 113: 243–4.

Sagnelli A, Piscosquito G, Chiapparini L, Ciano C, Salsano E, Saveri P, et al. X-linked Charcot-Marie-Tooth type 1: stroke-like presentation of a novel *GJB1* mutation. J Peripher Nerv Syst 2014; 19: 183–6.

Simpson MA, Cross H, Proukakis C, Pryde A, Hershberger R, Chatonnet A, et al. Maspardin is mutated in mast syndrome, a complicated form of Hereditary Spastic Paraplegia associated with dementia. Am J Hum Genet 2003; 73: 1147–56.

Spiegel R, Mandel H, Saada A, Lerer I, Burger A, Shaag A, et al. Delineation of *C12orf65*-related phenotypes: a genotype-phenotype relationship. Eur J Hum Genet 2014; 22: 1019–25.

Stevanin G, Santorelli FM, Azzedine H, Coutinho P, Chomilier J, Denora PS, et al. Mutations in SPG11, encoding spatacsin, are a major cause of spastic paraplegia with thin corpus callosum. Nat Genet 2007a; 39: 366–72.

Stevanin G, Azzedine H, Denora P, Boukhris A, Tazir M, Lossos A, et al. Mutations in SPG11 are frequent in autosomal recessive spastic paraplegia with thin corpus callosum, cognitive decline and lower motor neuron degeneration. Brain 2007b; 131: 772–84.

Tamiya G, Makino S, Hayashi M, Abe A, Numakura C, Ueki M, et al. A Mutation of *COX6A1* causes a recessive axonal or mixed form of Charcot-Marie-Tooth Disease. Am J Hum Genet 2014; 95: 294–300.

Tazir M, Bellatache M, Nouioua S, Vallat JM. Autosomal recessive Charcot-Marie-Tooth disease: from genes to phenotypes. J Peripher Nerv Syst 2013; 18: 113–29.

Tazir M, Hamadouche T, Nouioua S, Mathis S, Vallat JM. Hereditary motor and sensory neuropathies or Charcot-Marie-Tooth diseases: an update. J Neurol Sci 2014; 347: 14–22.

Tessa A, Denora PS, Racis L, Storti E, Orlacchio A, Santorelli FM. Bridging over the troubled heterogeneity of SPG-related pathologies: mechanisms unite what genetics divide [Review]. Curr Mol Med 2014; 14: 1034–42.

Tesson C, Nawara M, Salih MAM, Rossignol R, Zaki MS, Al Balwi M, et al. Alteration of fatty-acid-metabolizing enzymes affects mitochondrial form and function in hereditary spastic paraplegia. Am J Hum Genet 2012; 91: 1051–64.

Timmerman V, Clowes VE, Reid E. Overlapping molecular pathological themes link Charcot-Marie-Tooth neuropathies and hereditary spastic paraplegias [Review]. Exp Neurol 2013; 246: 14–25.

Van Goethem G, Dermaut B, Löfgren A, Martin JJ, Van Broeckhoven C. Mutation of *POLG* is associated with progressive external ophthalmoplegia characterized by mtDNA deletions. Nat Genet 2001; 28: 211–2.

Yum SW, Zhang J, Mo K, Li J, Scherer SS. A novel recessive *NEFL* mutation causes a severe, early-onset axonal neuropathy. Ann Neurol 2009; 66: 759–70.

Windpassinger C, Auer-Grumbach M, Irobi J, Patel H, Petek E, Hörl G, et al. Heterozygous missense mutations in *BSCL2* are associated with distal hereditary motor neuropathy and Silver syndrome. Nat Genet 2004; 36: 271–6.

Zimoń M1, Baets J, Almeida-Souza L, De Vriendt E, Nikodinovic J, Parman Y, et al., Loss-of-function mutations in *HINT1* cause axonal neuropathy with neuromyotonia. Nat Genet 2012: 44: 1080–3.